Spring 5-25-2018

A π-conjugated inorganic polymer constructed from boron difluoride formazanates and platinum(II) diynes

Jasveer S. Dhindsa

Ryan R. Maar

Stephanie M. Barbon

Maria Olivia Avilés

Zachary K. Powell

See next page for additional authors

Chemical Communications

COMMUNICATION

A π-conjugated inorganic polymer constructed from boron difluoride formazanates and platinum(II) diynes

Received 00th January 20xx,
Accepted 00th January 20xx

DOI: 10.1039/x0xx00000x

www.rsc.org/

Jasveer S. Dhindsa,[a] Ryan R. Maar,[a] Stephanie M. Barbon,[a] María Olivia Avilés,[a] Zachary K. Powell,[a] François Lagugné-Labarthet,[a] and Joe B. Gilroy*[a]

The first example of a π-conjugated polymer incorporating boron difluoride (BF_2) formazanates is introduced. The film-forming properties, controllable reduction chemistry, and low optical band gap (*ca.* 1.4 eV) of the polymer make it an excellent candidate for use as a light-harvesting *n*-type semiconductor in organic electronics. Comparison of the polymer to model compounds confirmed that its unique optoelectronic properties can be directly attributed to the presence of the BF_2 formazanate repeat unit and that the $[Pt(PBu_3)_2]^{2+}$ unit must also be present to achieve the narrow band gaps observed.

Polymers containing electron-deficient boron-containing subunits are a class of inorganic polymers that has received significant attention as a result of their use in a range of organic electronics and sensing technologies.[1,2] Platinum(II) polyynes incorporating a wide range of π-conjugated organic comonomers and electron-rich platinum(II) diyne units have received similar attention and have found application as the functional component of a variety of devices, including light-emitting diodes and photovoltaic cells.[3,4]

Although examples of molecular materials with unique optoelectronic properties have been produced by integrating both boron and platinum,[5] polymers containing both of these elements remain scarce throughout the literature.[6] Herein, we introduce a readily accessible π-conjugated polymer based on electron-poor boron difluoride (BF_2) formazanate and electron-rich platinum(II) diyne subunits as a promising candidate for use in organic electronics.

BF_2 formazanates are an emerging class of nitrogen-rich molecular materials that exhibit structurally tunable absorption, emission, and redox properties.[7] Their broad and red-shifted absorption characteristics and unusual ability to support stable radicals upon chemical reduction[8] differentiate them from related boron-dipyrromethenes (BODIPYs), and make them ideally suited for incorporation into *n*-type π-conjugated polymers. Their distinct properties arise from the presence of multiple nitrogen atoms within the BF_2 formazanate framework, which serve to enhance electronic delocalization, lower frontier orbital energies, and stabilize open shell species. Model compounds, which are the first molecular conjugates of platinum(II) diyne units with any formazanate-containing species, were prepared to facilitate an understanding of the optoelectronic properties of this intriguing new polymer type, including the effect of the presence/absence of the $[Pt(PBu_3)_2]^{2+}$ group in the π-conjugated polymer backbone.

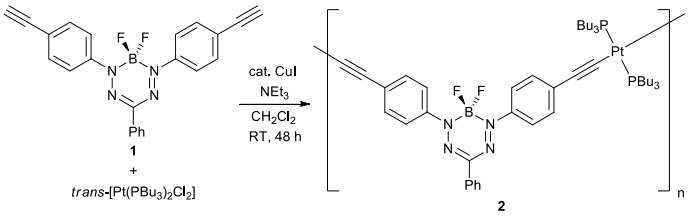

Scheme 1 Synthesis of polymer **2**.

The reaction of alkyne-functionalized BF_2 formazanate **1**[9] with *trans*-$[Pt(PBu_3)_2Cl_2]$[10] in the presence of catalytic CuI for 2 days produced polymer **2** (M_n = 20,430 g mol^{-1}, $Đ$ = 1.85) in 72% yield (Scheme 1, Figs. S1–S3). Polymer **2** can be heated without significant degradation up to temperatures of *ca.* 235 °C and no distinct glass transition was observed between

Chart 1 Model compounds **3–5**.

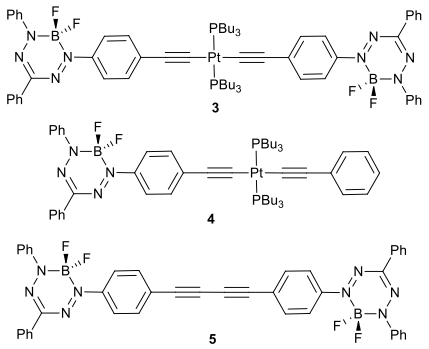

[a] Department of Chemistry and the Centre for Advanced Materials and Biomaterials Research (CAMBR), The University of Western Ontario, London, ON, Canada, N6A 5B7

Electronic Supplementary Information (ESI) available: Experimental details, NMR spectra, thermal analysis data, and thin-film AFM and UV-vis absorption spectroscopic data. See DOI: 10.1039/x0xx00000x

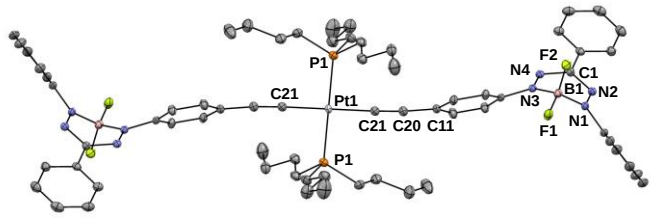

Fig. 1 Solid-state structure of **3**. Thermal displacement ellipsoids are shown at the 50% probability level and hydrogen atoms are removed for clarity. Selected bond lengths (Å): Pt1-P1 2.3026(7); Pt1-C21 1.9924(14); C21-C20 1.2170(19); N1-N2 1.3137(18); N3-N4 1.3122(17); N2-C1 1.3409(18); N4-C1 1.3504(17); N1-B1 1.554(2); N3-B1 1.5576(19). Selected bond angles (°): P1-Pt1-P1 180.0; Pt1-C21-C20 177.62(13); C21-C20-C11 174.28(16); N3-N4-C1 116.78(11); N4-C1-N2 123.01(12); N1-N2-C1 117.52(11); N3-B1-N1 100.04(12); F1-B1-F2 112.41(13).

–70 °C and 225 °C (Fig. S4). Similar reactions involving asymmetrically substituted precursors were employed to produce model compounds **3** and **4**, while Glaser coupling produced compound **5** (Chart 1, Figs. S5–S12).

The solid-state structure of **3** was examined as a model for the backbone of polymer **2** (Fig. 1). The Pt1 atom sits on a centre of inversion and the Pt1-C21 and C21-C20 bond lengths of 1.9924(14) Å and 1.2170(19) Å are consistent with those of discrete platinum(II) diyne complexes.[11] Notable metrics associated with the BF_2 formazanate unit include average N-N and C-N bond lengths of 1.3130(18) Å and 1.3457(18) Å, which indicate significant delocalization of the π-electrons within the formazanate ring. The *N*-aryl substituents are oriented in a fashion that should facilitate extended electronic delocalization, and the planes defined by these rings are offset by 46.4° and 50.4° compared to the plane defined by N1-N2-N3-N4. The 'dragonfly' conformation adopted by the BF_2 formazante is consistent with other discrete examples,[3c] and appears to arise as a result of the displacement of the boron atom by 0.63 Å from the N_4 plane.

As is often the case when platinum(II) diyne units are conjugated to electron deficient moieties,[12] degassed solutions of compounds **1–5** exhibit very weak photoluminescence (Φ_{PL} < 1%). Conversely, these compounds have rich absorption properties (Fig. 2a, Table 1). The low-energy absorption features of the spectra of related BF_2 formazanates have been shown to arise from electronic transitions dominated by the HOMO and LUMO orbitals,[3c] and are sensitive to the identity of the substituent at the *para*-position of the *N*-aryl rings.[3b] Consistent with these observations, the lowest-energy bands observed were responsive to the degree of extended electronic delocalization associated with the *N*-aryl ring and the wavelength of maximum absorption (λ_{max}) red-shifted as the size of the π-system increased from 541 nm (ε = 27,700 M^{-1} cm^{-1}) for **1** to 588 nm (ε = 20,000 M^{-1} cm^{-1}) and 598 nm (ε = 77,400 M^{-1} cm^{-1}) for compounds **4** and **3**, and finally 661 nm (ε = 45,500 M^{-1} cm^{-1}) for polymer **2**. A uniform film of **2** spin-coated from chlorobenzene gave rise to a broadened, red-shifted absorption band (λ_{max} = 680 nm, Fig. S13). Direct comparison of models **3** and **4** allowed for the conclusion that electronic delocalization extends through the electron-rich $[Pt(PBu_3)_2]^{2+}$ unit. Similarly, the absorption properties of models **3** and **5** [564 nm (ε = 57,100 M^{-1} cm^{-1})] confirm that the Pt(II) centre plays a critical role in reducing the optical band gap (E_g) in this series of complexes, which was estimated as 1.5 eV and 1.4 eV in solution and thin-film for polymer **2** (Fig. S13, Table 1). The narrow optical band gap observed for **2** results from the advantageous properties of the

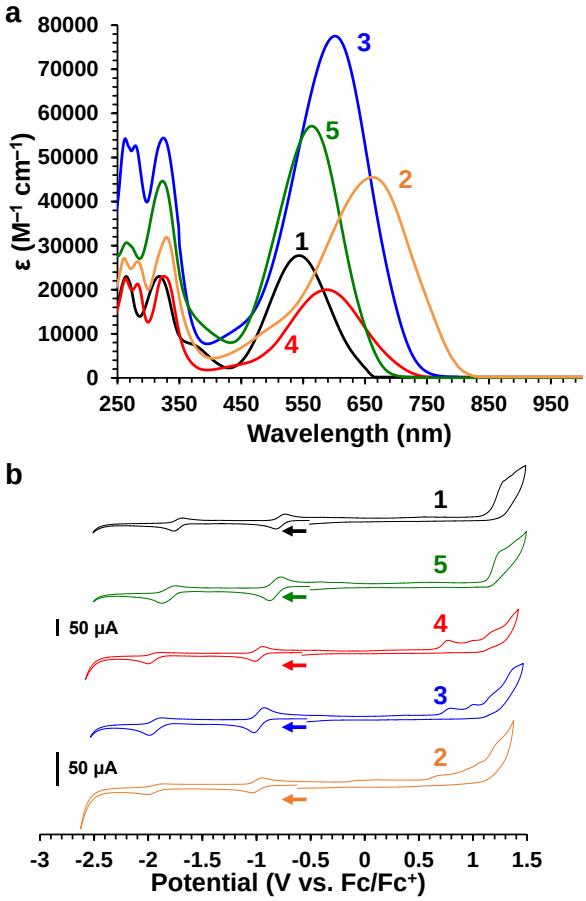

Fig. 2 (a) UV-vis absorption spectra recorded for compounds **1–5** in CH_2Cl_2. (b) Cyclic voltammograms recorded for compounds **1–5** (1 mM) at 250 mV s^{-1} in CH_2Cl_2 containing 0.1 M [nBu$_4$N][PF_6] as supporting electrolyte. The lower current response observed for polymer **2** is a result of its poor diffusion characteristics at the working electrode interface.

Table 1 Solution phase spectroscopic and electrochemical data obtained for compounds **1–5** in CH_2Cl_2.

	λ_{max} (nm)	ε (M^{-1} cm^{-1})	E_g (eV)[a]	E_{red1} (V vs. Fc/Fc^+)	E_{red2} (V vs. Fc/Fc^+)	E_{ox1} (V vs. Fc/Fc^+)[b]	E_{ox2} (V vs. Fc/Fc^+)[b]	E_{ox3} (V vs. Fc/Fc^+)[b]
1	541	27,700	1.86	–0.78	–1.73	-	-	1.27
2	661	45,500[c]	1.49	–1.00	–1.94	0.71	1.06	1.23
3	598	77,400	1.59	–0.96	–1.91	0.76	1.02	1.16
4	588	20,000	1.66	–0.97	–1.94	0.77	0.98	1.17
5	564	57,100	1.75	–0.83	–1.82	-	-	1.23

[a]Determined as the onset of the lowest-energy absorption. [b]Irreversible process, potential at maximum anodic current reported. [c]The molar absorptivity (ε) values reported for polymer **2** were calculated using the molecular weight of the repeating unit.

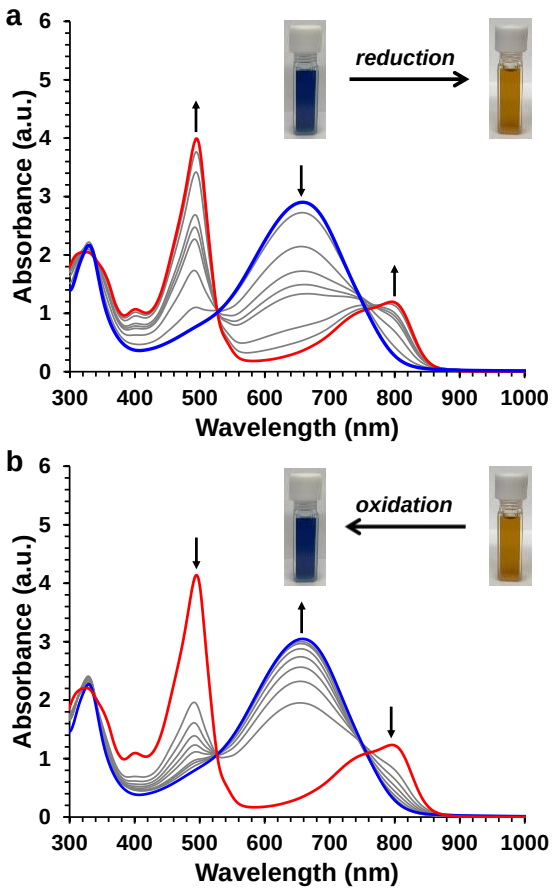

Fig. 3 UV-vis absorbance spectra recorded for a 80 μM solution of polymer **2** (blue line) and the fully reduced form of polymer **2** (1.5 equiv. cobaltocene, red line) in a 1:1 (v/v) mixture of CH_3CN and CH_2Cl_2. The grey lines in panel (a) are spectra recorded upon mixing polymer **2** with 0.25, 0.50, 0.75, 0.88, 0.95, 1.00, and 1.25 equiv. of cobaltocene. The grey lines in panel (b) are spectra recorded at time intervals of 1, 5, 9, 13, 17, 25, 37, and 45 min after a solution of the reduced form of polymer **2** was exposed to air. The spectrum recorded after 45 min was a quantitative match with that of polymer **2**. The vertical arrows denote the trends observed upon (a) reduction and (b) oxidation.

BF_2 formazanate repeat unit, and is significantly lower than that determined for the only known BODIPY/platinum(II) diyne polymer (1.7 eV).[6b]

Cyclic voltammograms (CVs) recorded for compounds **1–5** are shown in Fig. 2b and the data are summarized in Table 1. The simplest example, compound **1**, can be reduced in two, one-electron steps (E_{red1} = –0.78 V and E_{red2} = –1.73 V relative to the ferrocene/ferrocenium redox couple) to the corresponding radical anion and dianion (*i.e.*, **1** → $\mathbf{1}^{\bullet-}$ and $\mathbf{1}^{\bullet-}$ → $\mathbf{1}^{2-}$). It can also be irreversibly oxidized near the edge of the solvent window (E_{ox3} = 1.27 V). Comparison with the CV of **5** indicates that the BF_2 formazanate ring has become more electron-rich upon dimerization as both the reduction and oxidation features have shifted to more negative potentials. The current response associated with reduction also doubled due to the presence of two BF_2 formazanate units per mole of **5**. Incorporation of the electron-rich $[Pt(PBu_3)_2]^{2+}$ group in model compounds **3** and **4** further shifted each of the reduction/oxidation waves in the negative direction and introduced two new irreversible waves (E_{ox1} and E_{ox2}) associated with the stepwise oxidation of platinum(II).[13] Polymer **2** is the most difficult compound in this series to reduce and its CV was comprised of broadened reduction (E_{red1} = –1.00 V and E_{red2} = –1.94 V) and oxidation (E_{ox1} = 0.71 V, E_{ox2} = 1.06 V, and E_{ox3} = 1.23 V) features that are consistent with those of each of the repeating units present.[14] An additional broad oxidation feature was reproducibly observed between –0.15 V and 0.25 V.[15]

Given the unique optoelectronic properties afforded by the BF_2 formazanate repeating unit, we performed a stepwise chemical reduction of polymer **2** (Fig. 3a) and monitored the reaction using UV-vis absorption spectroscopy. Upon addition of cobaltocene, the low-energy absorption band associated with polymer **2** (λ_{max} = 661 nm) began to disappear and two new maxima appeared at 495 nm and 795 nm. The spectrum obtained for the fully reduced polymer was red-shifted, but qualitatively similar to those reported for formazanate-based radical anions derived from related molecular species.[8] The thin-film absorption spectrum acquired for the reduced form of polymer **2** shared similar, broadened features (Fig. S14). Electron paramagnetic resonance (EPR) spectroscopy of the same polymer in a 1:20 (v/v) mixture of CH_3CN and CH_2Cl_2 (290 μM) yielded a broad isotropic signal centred at g = 2.0042 that was consistent with the formation of a poly(radical anion) (Fig. S14). The chemical reduction process was demonstrated to be completely reversible by exposing a solution of the reduced form of polymer **2** to air (Fig. 3b). After 1 min, approximately 50% of the radical anion repeat units derived from BF_2 formazanates had converted to their neutral form and complete conversion to polymer **2** was observed after 45 min. The stepwise control and reversibility of the reduction process demonstrated by these studies sets the stage for the use of polymer **2** as a light-harvesting *n*-type material whereby controlled degrees of doping may be used to optimize performance.

In conclusion, we have synthesized a rare example of a polymer containing both transition metal and main group elements. By examining a series of model compounds, we demonstrated that the distinctive optoelectronic properties of polymer **2** can be directly attributed to the presence of the BF_2 formazanate repeat unit and that the $[Pt(PBu_3)_2]^{2+}$ fragment is also an essential structural component with respect to the narrow band gaps observed. Given the relatively straightforward synthesis, narrow band gap, advantageous film-forming properties, and reversible electron-accepting ability of the polymer, it is likely to receive considerable attention from those pursuing next-generation organic electronics. Our future efforts will focus on establishing a small library of analogous polymers and examining their properties, including *n*-type semiconductivity in the solid state.

This work was supported by the Natural Sciences and Engineering Research Council (NSERC) of Canada (J.B.G.: DG, RGPIN-2013-435675, F.L.-L: DG, RGPIN-2015-04298, R.R.M. and S.M.B.: CGS-D Scholarships), the Ontario Ministry of Research and Innovation (J.B.G.: ERA, ER-14-10-147), and the

Canadian Foundation for Innovation (J.B.G.: JELF, 33977). The authors thank Dr. Paul Bazylewski and Dr. Giovanni Fanchini for assistance with EPR spectroscopy and access to instrumentation.

Conflicts of interest

There are no conflicts to declare.

Notes and references

1 Selected reviews: (a) F. Jäkle, *Chem. Rev.*, 2010, **110**, 3985; (b) K. Tanaka and Y. Chujo, *Macromol. Rapid Commun.*, 2012, **33**, 1235; (c) H. Helten, *Chem. Eur. J.*, 2016, **22**, 12972.

2 Selected examples: (a) B. Kim, B. Ma, V. R. Donuru, H. Liu and J. M. J. Fréchet, *Chem. Commun.*, 2010, **46**, 4148; (b) I. A. Adams and P. A. Rupar, *Macromol. Rapid Commun.*, 2015, **36**, 1336; (c) A. Hirose, K. Tanaka, R. Yoshii and Y. Chujo, *Polym. Chem.*, 2015, **6**, 5590; (d) C. Dou, X. Long, Z. Ding, Z. Xie, J. Liu and L. Wang, *Angew. Chem. Int. Ed.*, 2016, **55**, 1436; (e) J. Winsberg, T. Hagemann, S. Muench, C. Friebe, B. Häupler, T. Janoschka, S. Morgenstern, M. D. Hager and U. S. Schubert, *Chem. Mater.*, 2016, **28**, 3401; (f) T. Lorenz, M. Crumbach, T. Eckert, A. Lik and H. Helten, *Angew. Chem. Int. Ed.*, 2017, **56**, 2780; (g) B. Meng, Y. Ren, J. Liu, F. Jäkle and L. Wang, *Angew. Chem. Int. Ed.*, 2018, **57**, 2183.

3 Selected reviews: (a) W. Wang and H.-B. Yang, *Chem. Commun.*, 2014, **50**, 5171; (b) C.-L. Ho, Z.-Q. Yu and W.-Y. Wong, *Chem. Soc. Rev.*, 2016, **45**, 5264; (c) P. D. Harvey, *J. Inorg. Organomet. Polym.*, 2017, **27**, S3.

4 Selected examples: (a) W.-Y. Wong, X.-Z. Wang, Z. He, A. B. Djurišić, C.-T. Yip, K.-Y. Cheung, H. Wang, C. S. K. Mak and W.-K. Chan, *Nat. Mater.*, 2007, **6**, 521; (b) T. Kenny, S. M. Aly, D. Fortin and P. D. Harvey, *Chem. Commun.*, 2012, **48**, 11543; (c) A. K. Mahrok, E. I. Carrera, A. J. Tilley, S. Ye and D. S. Seferos, *Chem. Commun.*, 2015, **51**, 5475; (d) C.-H. Siu, L. T. L. Lee, S.-C. Yiu, P.-Y. Ho, P. Zhou, C.-L. Ho, T. Chen, J. Liu, K. Han and W.-Y. Wong, *Chem. Eur. J.*, 2016, **22**, 3750; (e) Z. Meng, G. Li, H.-F. Wong, S.-M. Ng, S.-C. Yiu, C.-L. Ho, C.-W. Leung, I. Manners and W.-Y. Wong, *Nanoscale*, 2017, **9**, 731.

5 Selected examples: (a) N. Wang, S.-B. Ko, J.-S. Lu, L. D. Chen and S. Wang, *Chem. Eur. J.*, 2013, **19**, 5314; (b) L. Liu, S. Guo, J. Ma, K. Xu, J. Zhao and T. Zhang, *Chem. Eur. J.*, 2014, **20**, 14282; (c) H. Braunschweig, A. Damme, R. D. Dewhurst, H.Kelch, B. B. Macha, K. Radacki, A. Vargas and Q. Ye, *Chem. Eur. J.*, 2015, **21**, 2377; (d) W. Yang, A. Karatay, J. Zhao, J. Song, L. Zhao, Y. Xing, C. Zhang, C. He, H. G. Yaglioglu, M. Hayvali, A. Elmali and B. Küçüköz, *Inorg. Chem.*, 2015, **54**, 7492; (e) H. Lei, S. M. Aly, P.-L. Karsenti, D. Fortin and P. D. Harvey, *Inorg. Chem.*, 2017, **56**, 13140; (f) P. Wang, Y. H. Koo, W. Kim, W. Yang, X. Cui, W. Ji, J. Zhao and D. Kim, *J. Phys. Chem. C*, 2017, **121**, 11117.

6 (a) F. Matsumoto, N. Matsumi and Y. Chujo, *Polym. Bull.*, 2001, **46**, 257; (b) W. He, Y. Jiang and Y. Qin, *Polym. Chem.*, 2014, **5**, 1298.

7 (a) S. M. Barbon, P. A. Reinkeluers, J. T. Price, V. N. Staroverov and J. B. Gilroy, *Chem. Eur. J.*, 2014, **20**, 11340; (b) S. M. Barbon, J. T. Price, P. A. Reinkeluers and J. B. Gilroy, *Inorg. Chem.*, 2014, **53**, 10585; (c) R. R. Maar, S. M. Barbon, N. Sharma, H. Groom, L. G. Luyt and J. B. Gilroy, *Chem. Eur. J.*, 2015, **21**, 15589; (d) S. M. Barbon, V. N. Staroverov and J. B. Gilroy, *J. Org. Chem.*, 2015, **80**, 5226.

8 (a) M.-C. Chang and E. Otten, *Chem. Commun.*, 2014, **50**, 7431; (b) S. M. Barbon, V. N. Staroverov and J. B. Gilroy, *Angew. Chem. Int. Ed.*, 2017, **56**, 8173.

9 S. M. Barbon and J. B. Gilroy, *Polym. Chem.*, 2016, **7**, 3589.

10 G. B. Kauffman, L. A. Teter and J. E. Huheey, *Inorg. Synth.*, 1963, **7**, 245.

11 T. B. Peters, Q. Zheng, J. Stahl, J. C. Bohling, A. M. Arif, F. Hampel and J. A. Gladysz, *J. Organomet. Chem.*, 2002, **641**, 53.

12 C.-L. Ho and W.-Y. Wong, *Coord. Chem. Rev.*, 2013, **257**, 1614.

13 M. Younus, A. Köhler, S. Cron, N. Chawdhury, M. R. A. Al-Mandhary, M. S. Khan, J. Lewis, N. J. Long, R. H. Friend and P. R. Raithby, *Angew. Chem. Int. Ed.*, 1998, **37**, 3036.

14 Aged samples of polymer **2** exhibit a third reduction feature at *ca.* E_{pc} = –1.5 V vs. Fc/Fc^{+}. The appearance of this feature was not accompanied by the appearance of a new signal in related NMR spectra.

15 The broad oxidation features observed for polymer **2** did not allow for an accurate estimate of the HOMO energy to be made. We therefore have not included a comparison of the optical and electrochemical band gaps.

